FREESTANDING SOLID-STATE MICRO-SUPERCAPACITOR BASED ON LASER-PATTERNED NANOFIBERS

Yu Song[1], Xuexian Chen[1,2], Haotian Chen[1,2], Xiaoliang Cheng[1], Jinxin Zhang[1], Zongming Su[1], Liming Miao[1], Bo Meng[4], Quan Yuan[3,] and Haixia Zhang[1,2,*]*

[1]National Key Laboratory of Science and Technology on Micro/Nano Fabrication, Institute of Microelectronics, Peking University, Beijing, CHINA

[2]Academy for Advanced Interdisciplinary Studies, Peking University, Beijing, CHINA

[3]Institute of Semiconductors, Chinese Academy of Sciences, Beijing, CHINA

[4]Beijing Micro Energy Technology Co., Ltd, Beijing, CHINA

ABSTRACT

In this paper, we present a novel fabrication for freestanding solid-state micro-supercapacitor (MSC) with interdigital carbon nanotube (CNT)/nanofibers electrode layer, gold current collector and the solid-state electrolyte-substrate, which, for the first time, combines electrolyte transferring with laser patterning process. With the in-planar electrode and electrolyte-substrate layout, the dimension of MSC could be greatly decreased. Meanwhile, taking advantage of electrospinning nanofibers with large surface-area and CNTs with high conductivity, the line-width finger (200 μm) of MSC exhibits high areal capacitance (15.6 mF/cm^2), good energy and power density. In addition, the capacitance retention retains more than 83% after 2,000 cycles which performs stable and excellent electrochemical performance. Therefore, such flexible freestanding MSC shows great potentials to satisfy the requirements of miniaturized energy systems and wearable devices.

INTRODUCTION

With the rapid development of portable electronics, the technology of highly integrated electronic systems has been significantly advanced [1, 2]. Harvesting energy from the environment from the environment such as triboelectric nanogenerator [3, 4], piezoelectric nanogenerator [5, 6] is a considerable approach. At the same time, besides various nanogenerators, high performance energy storage devices, as another critical component in power systems, are also in great demands [7]. Among the presently available energy storage devices, supercapacitors is a promising state-of-the-art device, filling the blank between the battery with high specific energy density and the conventional capacitor with high specific power density. Supercapacitor is considered to have high application potentials attributed to its long cycle lifetime, fast charging/discharging rates and great stability.

Recently, the emergence of in-planar supercapacitor [10, 11], also called micro-supercapacitor is regarded as a significant member in the family of miniaturized energy storage devices, which has drawn great attentions in energy fields. Compared with the normal supercapacitor which owns sandwiched structure [12], such in-planar layout can render the diffusion length and promote the procedure of ion exchange. Independent to the electrode thickness, MSC could allow more active materials loaded per unit area and maintain excellent electrochemical performance at the same time. More importantly, owing to the in-planar layout and elimination of the separator [13], the total thickness of the device could be greatly decreased, showing capable candidates in microelectronic power systems [14].

However, due to the fact that most of MSCs are commonly employed with lithography process [15], it has proved costly and awkward in developing energy-storage devices, which could possibly damage and corrode the electrode materials during the etching stage. In addition, the process is complicated by transferring the electrodes from a rigid substrate to a flexible substrate which brings in excess substrate to further increase the whole thickness and destroys the device integrity to some extent [16].

In order to address the above issues, we present an interdigital freestanding MSC through the electrolyte transferring and laser patterning process in this paper. Without excess substrate, the total thickness could be further reduced and the flexibility also could be great enhanced. Additionally, without the lithography process and use of shadow mask, such the process could simplify the scalable and integrated fabrication, which have significant impacts on micro-energy storage devices.

EXPERIMENTAL METHODS

Schematic diagram of the MSC is shown in Fig. 1, which includes the electrospinning nanofibers, flexible electrode, current collector and solid-state electrolyte. It is worth mentioning that the electrolyte also serves as the substrate and interdigital electrodes composing CNTs serve as anode and cathode. The whole device weighs only 20 mg, which performs good flexibility and portability.

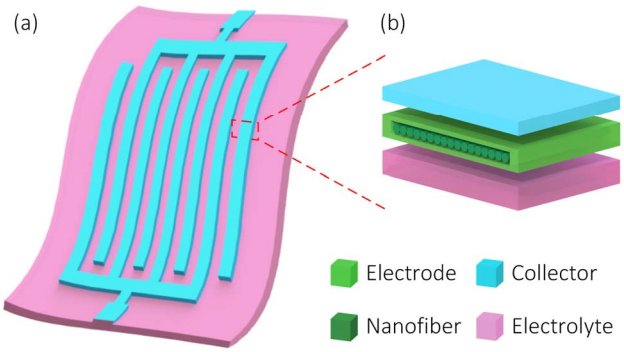

Figure 1: Schematic diagram of the freestanding MSC. (a) Flexible view, and (b) exploded view of the structure.

Material preparation

The preparation of the polymer solution is essential for the electrospinning process. In our process, 1 g of polyvinylidene fluoride (PVDF, Kureha) is dissolved in

dimethyl formamide (DMF)/acetone (Sigma Aldrich) mixtures at a polymer/solvent concentration of 10% w/w and the mixture is subsequently magnetic stirred for 8 h at the room temperature until the solution becomes homogeneous and transparent.

The CNT ink solution is prepared by dispersing 60 mg of CNTs with 60 mg of sodium dodecylbenzenesulfonate (SDBS) surfactant in 60 ml of deionized water and bath-sonicated for 4 h to disperse evenly. Then solid-state electrolyte is prepared by adding polyvinyl alcohol (PVA) powder (6 g) into H_3PO_4 aqueous solution (6 g H_3PO_4 into 60 ml deionized water). The whole mixture is heated to 85°C under vigorous stirring until the solution becomes clear.

Fabrication of MSC device

The fabrication process of the MSC device is demonstrated in Fig. 2. Firstly, it begins by electrospinning PVDF nanofibers with large surface area, which is performed by placing 0.9 ml of PVDF solution into a 1.0 ml plastic syringe with a blunt-tip needle. With the needle placed 8 cm away from the collector and charged at a bias voltage of 10 kV, the solution is fed up at a constant speed of 1 ml/h. Under such high voltage, the polymer solution is ejected and finally collected by the substrate.

Then CNT ink solution is dropped on the nanofibers and dried at 90°C for several times until the CNT is saturated in the nanofibers as the active materials. Next, gel electrolyte consisting of PVA and H_3PO_4 is spray coated on the CNT-nanofiber electrodes. The device is completely dried in a regular oven at 45°C for 12 h to fully vaporize the excess water. After the above layers is peeled off from the PET substrate mechanically, the electrodes are easily transferred to the electrolyte film without further substrate.

To efficiently promote the charge flow, Au (100 nm) is sputtered beyond the electrodes as current collector via magnetron sputtering process. Finally, the electrodes and current collector are patterned into interdigital structure by laser-cutting process, and the freestanding MSC is successfully prepared.

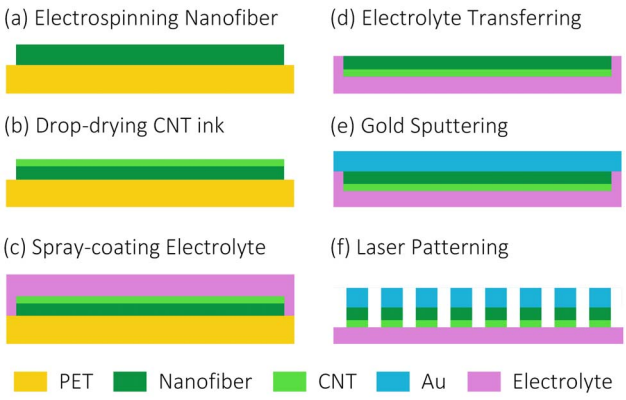

Figure 2: Fabrication process of the freestanding MSC. (a) Depositing nanofiber electrospinning on the PET substrate, (b) drop-drying CNT ink on the nanofibers, (c) spray-coating electrolyte on the electrodes, (d) transferring the electrodes by the electrolyte, (e) sputtering the gold as the current collector, and (f) patterning the electrode by laser cutting process.

Measurement and Analysis

The morphologies, structure of each layer and the interdigital MSC are all analyzed using a scanning electron microscope (SEM) (Quanta 600F, FEI Co.). All of the electrochemical tests of the freestanding MSC are carried out by a two-electrode system using CHI660C (CH instrument) electrochemical workstation at room temperature.

RESULTS AND DISCUSSION

Optical and SEM analysis

Using the proposed process, the freestanding MSC with patterned electrodes has been fabricated shown in Fig. 3a, the side length of which is 1 cm. From the optical microscopic image in Fig. 3b, it clearly demonstrates that the electrodes of the MSC have a well-defined shape and sharp boundaries. In addition, SEM images in Fig. 3c-3e clearly demonstrate the morphologies of every process, where the nanofibers are freely electrospun in the substrate, CNTs are uniformly coated among the nanofibers and conformal gold layer is deposited as the current collector, respectively. The cross-section SEM image of the device in Fig. 3d shows each finger contains two layers, which are solid-state electrolyte film and electrode layer from the bottom to the top. Here, the electrolyte is penetrated into the electrode, thus enhancing the ion exchange greatly (Fig. 3f).

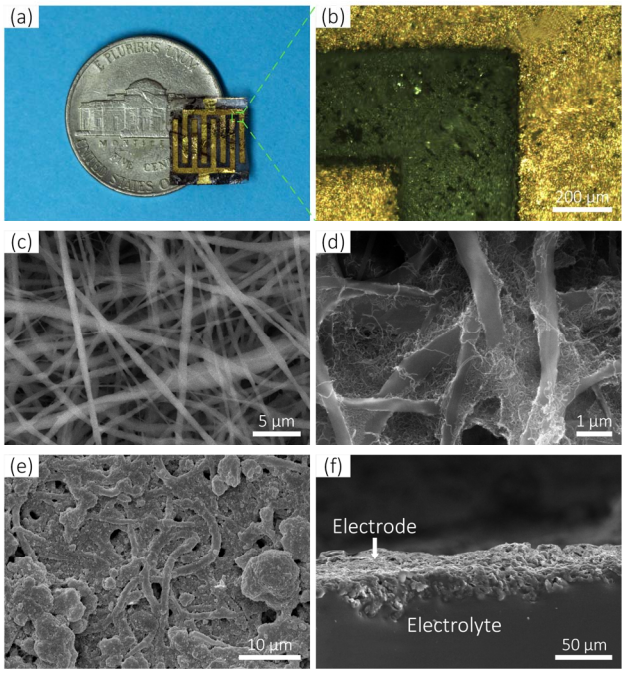

Figure 3: (a) Digital image and (b) Microscopic image of the device. SEM image of (c) electrospinning nanofibers, (d) CNT coated nanofibers, (e) gold sputtered electrodes and (f) the cross-section of the device.

To investigate the relationship between electrochemical performance and the line-width, MSC with 200 µm line-width of finger (defined as MSC 200) is designed. The inter-space of the interdigital finger is kept for a value of 400 µm. The structure in Fig. 4a stands for the designed MSC unit and the meanings of each symbol, where each interdigital electrode has 4 fingers.

Additionally, the Fig. 4b includes the detailed parameter of each symbol and the whole area and volume of each MSC 200 device.

(a)

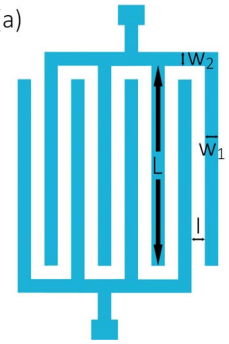

(b)

Parameter	MSC 200
W_1 (μm)	200
W_2 (μm)	200
l (μm)	400
L (μm)	6000
Total S (cm^2)	0.1328
Total V ($\times 10^{-4}$ cm^3)	5.312

Figure 4: (a) Structure and (b) detailed parameter of designed micro-electrodes.

Electrochemical analysis

Afterwards, in order to further explore the electrochemical performance of the freestanding MSC, the device is carefully evaluated through cyclic voltammetry (CV), galvanostatic charge-discharge (GCD), Ragone plots and cycling stability via the electrochemical workstation. Firstly, with the effective area of 0.1328 cm^2, the MSC is analyzed by CV curves with the scan rates from 10 mV/s to 200 mV/s at a stable potential window between 0 and 1 V (Fig. 5a). Definitely, the CV curves retain quasi-rectangular shape and are approximately symmetrical about the zero-current line, thus indicating the ideal double-layer electrochemical behavior.

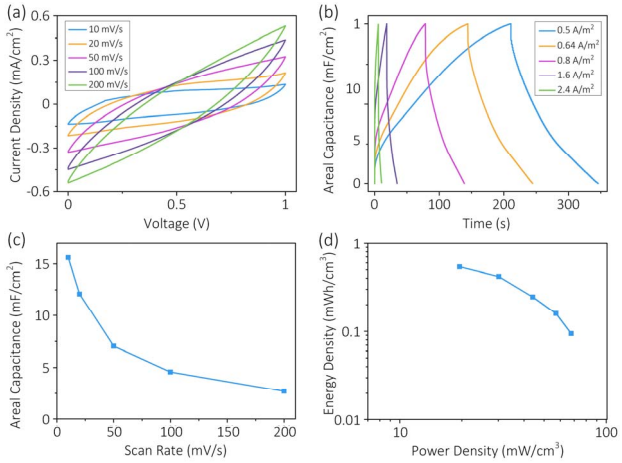

Figure 5: Electrochemical behavior of the MSC 200. (a) CV curves, (b) GCD curves, (c) calculated areal capacitance and (d) Ragone plot of the device.

Then GCD test is also carried out to further evaluate the electrochemical performance of freestanding MSC. As shown in Fig. 5b, the typical GCD curves are performed, the charging-discharging current densities of which are from 0.5 A/m^2 to 2.4 A/m^2. Discharging profiles of the fabricated MSC are dependent on the applied charging-discharging current densities and similar curve shapes have been obtained for different current densities. Evidently, GCD curves could reveal that all of the charging curves are symmetrical with their corresponding discharging counterparts, as well as their excellent linear voltage-time profiles, demonstrating good electrochemical behavior of the device.

Besides, the areal capacitance is achieved according to the following equations with the CV curves of the freestanding MSC:

$$C_A = \frac{Q}{A \cdot \Delta V} = \frac{1}{\mathrm{k} \cdot A \cdot \Delta V} \int_{V_1}^{V_2} I(V) dV \qquad (1)$$

where, C_A is the areal capacitance, $I(V)$ is the discharge current function, k is the scan rate, A is the area of the MSC and ΔV is the potential window during the discharge process, where V_1 and V_2 are maximum and minimum voltage values, respectively. With the scan rate of the MSC at the 10 mV/s, the MSC could achieves the maximum areal capacitance of 15.6 mF/cm^2, which decreases slightly with the increase of the scan rate (Fig. 5c). As a result, such MSC device could withstand the charging-discharging process without significant degradation in areal capacitance even at high scan rate, showing a stable and excellent electrochemical performance.

The volumetric energy and power density of the MSC are calculated from CV curves at a voltage scan rate of 10 to 200 mV/s, and shown in Fig. 5d. Both of the energy and power density of the MSC device at initial state could be achieved by the following equations with the volume of 5.312×10^{-4} cm^3:

$$C_V = \frac{Q}{V \cdot \Delta V} = \frac{1}{\mathrm{k} \cdot V \cdot \Delta V} \int_{V_1}^{V_2} I(V) dV \qquad (2)$$

$$E = \frac{1}{2 \times 3600} C_V (\Delta V)^2 \qquad (3)$$

$$P = \frac{E}{\Delta t} \times 3600 \qquad (4)$$

where, C_V is the volumetric capacitance of the MSC which can be achieved through eq. 2, Δt is the discharging time, E is the energy density and P is the power density, respectively. The highest energy density of the MSC is 0.54 mWh/cm^3 at the scan rate of 10 mV/s, at the same time, the highest power density is 67.7 mW/cm^3 at the scan rate of 200 mV/s, respectively. Definitely, both of them vary slightly with the increase of scan rates.

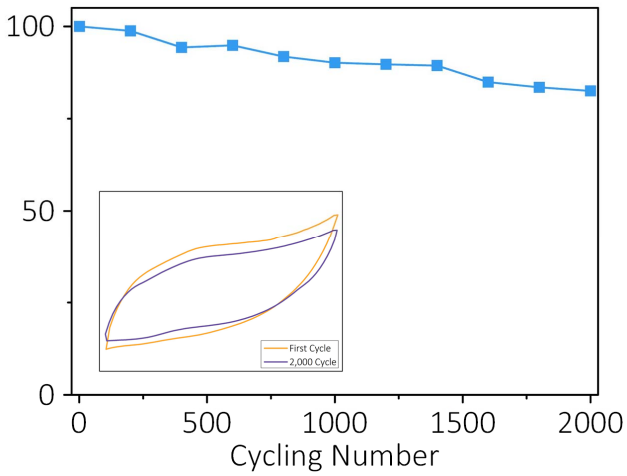

Figure 6: Cycling stability of the MSC 200; (inset) the CV curves recorded during the cycling process.

Fig. 6 shows the capacitance retention of the MSC

with interdigital electrodes during the repetitive charge/discharge cycles. It is evident that about 83% of the initial capacitance is maintained after 2,000 cycles of CV tests. The inset of Fig. 6 demonstrates the typical CV curves of the first and last cycles, exhibiting the stable quasi-rectangular shape. Therefore, the cycling stability and relative electrochemical tests of the freestanding MSC indicates that the MSC device owns stable and excellent electrochemical performance, which could satisfy the needs of the flexible electronics and self-powered systems.

CONCLUSIONS

In summary, we propose a facile and scalable procedure for fabricating a freestanding solid-state MSC with superior characteristics of lightweight, flexibility, stabilization and excellent electrochemical performance. Combing the electrolyte transferring with laser patterning process, such MSC device is configured with CNT/nanofibers as interdigital electrodes, gold layer as current collector and PVA/H_3PO_4 as the solid-state electrolyte and substrate. With the in-planar and electrolyte-substrate layout, the dimension of MSC could be greatly decreased. The entire device demonstrates excellent electrochemical behavior with a high capacitance and stability cycling performance according to the fact that the electrospinning nanofibers own large surface area and CNTs exhibit high conductivity. Furthermore, MSC device could be further enhanced by optimizing the line-width of finger and designing serial or parallel connection to broaden its working range. Therefore, such freestanding MSC performs significant advantages in MEMS-based technology, large-scale fabrication and low-cost electronics, as well as wearable devices and flexible miniaturized energy systems.

ACKNOWLEDGEMENTS

This work is supported by the National Natural Science Foundation of China (Grant No. 61674004, 61176103, 91323304 and 61404136), National Key R&D Project from Ministry of Science and Technology, China (2016YFA0202701), and the Beijing Science & Technology Project (Grant No. Z141100003814003) and the Beijing Natural Science Foundation of China (Grant No. 4141002).

REFERENCES

[1] Z. Wang, "Self-Powered Nanosensors and Nanosystems", *Adv. Mater.*, vol. 24, pp. 280-285, 2012.

[2] Y. Song, X. Cheng, H. Chen, J. Huang, X. Chen, M. Han, Z. Su, B. Meng, Z. Song and H. Zhang, "Integrated self-charging power unit with flexible supercapacitor and triboelectric nanogenerator", *J. Mater. Chem. A*, vol. 4, pp. 14298-14306, 2016.

[3] F. Fan, Z. Tian, Z. Wang, "Flexible triboelectric generator", *Nano Energy*, vol. 1, pp. 328-334.

[4] X. Cheng, B. Meng, X. Chen, M. Han, H. Chen, Z. Su, M. Shi and H. Zhang, "Single-Step Fluorocarbon Plasma Treatment-Induced Wrinkle Structure for High-Performance Triboelectric Nanogenerator", *Small*, vol. 12, pp. 229-236, 2016.

[5] M. Han, X. Zhang, B. Meng, W. Liu, W. Tang, X. Sun, W. Wang and H. Zhang, "r-Shaped hybrid nanogenerator with enhanced piezoelectricity", *ACS Nano*, vol. 7, pp. 8554-8560, 2013.

[6] S. Cha, J. Seo, S. Kim, H. Kim, Y. Park, S. Kim and J. Kim, "Sound-Driven Piezoelectric Nanowire-Based Nanogenerators", *Adv. Mater.*, vol. 22, pp. 4726-4730, 2010.

[7] P. Simon and Y. Gogotsi, "Materials for electrochemical capacitors", *Nature Mater.*, vol. 7, pp. 845-854, 2008.

[8] X. Lu, M. Yu, T. Zhai, G. Wang, S. Xie, T. Liu, C. Liang, Y. Tong and Y. Li, "High energy density asymmetric quasi-solid-state supercapacitor based on porous vanadium nitride nanowire anode", *Nano Lett.*, vol. 13, pp. 2628–2633, 2013.

[9] X. Lu, M. Yu, G. Wang, Y. Tong and Y. Li, "Flexible solid-state supercapacitors: design, fabrication and applications", *Energy Environ. Sci.*, vol. 7, pp. 2160–2181, 2014.

[10] K. Wang, W. Zou, B. Quan, A. Yu, H. Wu, P. Jiang and Z. Wei, "An All-Solid-State Flexible Micro-supercapacitor on a Chip", *Adv. Energy Mater.*, vol. 1, pp. 1068-1072, 2011.

[11] C. Shen, G. Luo, A. Kozinda, M. Sanghadasa and L. Lin, "Solid-State Flexible Micro Supercapacitors by Direct-Write Porous Nanofibers", *Proc. MEMS 2015*, pp. 1133-1136.

[12] Y. Song, X. Cheng, H. Chen, M. Han, X. Chen, J. Huang, Z. Su and H. Zhang, "Highly compression-tolerant folded carbon nanotube/paper as solid-state supercapacitor electrode", *Micro & Nano Lett.*, vol. 11, pp. 586-590, 2016.

[13] S. Li, X. Wang, H. Xing, and C. Shen, "Micro supercapacitors based on a 3D structure with symmetric graphene or activated carbon electrodes", *J. Micromech. Microeng.*, vol. 23, pp. 114013, 2013.

[14] J. Luo, F. Fan, T. Jiang, Z. Wang, W. Tang, C. Zhang, M. Liu, G. Cao and Z. Wang, "Flexible self-charging power unit by integrating microsupercapacitor and triboelectric nanogenerator", *Nano Res.*, vol. 8, pp. 3934-3943, 2015.

[15] J. Yun, Y. Lim, G. Jang, D. Kim, S. Lee, S. Hong, G. Lee, G. Zi, and J. Ha, "Stretchable patterned graphene gas sensor driven by integrated micro-supercapacitor array", *Nano Energy*, vol. 19, pp. 401-414, 2016.

[16] M. Kim, B. Hsia, C. Carraro, and R. Maboudian, "Flexible micro-supercapacitors from photoresist-derived carbon electrodes on flexible substrates", *Proc. MEMS 2014*, pp. 389–392.

CONTACT

*Q. Yuan, yuanquan@semi.ac.cn;
*H.X. Zhang, hxzhang@pku.edu.cn